Density Functional Calculations of ^{3}He Chemical Shift in Endohedral Helium Fullerenes: Neutral, Anionic, and Di-Helium Species

Michal Straka* and Juha Vaara

Laboratory of Physical Chemistry, Department of Chemistry, University of Helsinki, P.O. Box 55 (A. I. Virtasen aukio 1), FIN-00014, Helsinki, Finland

Received: June 22, 2006; In Final Form: August 14, 2006

We report density functional calculations of ^{3}He nuclear magnetic resonance chemical shifts in a series of experimentally known endohedral helium fullerenes, $He_n@C_m{}^q$ (n = 1, 2; m = 60, 70, 76, 78; q = 0, 6−), including for the first time anionic and di-helium species. Despite the lack of dispersion in the density functional model, the results are in promising agreement with experiment. Density functional theory performs better than Hartree−Fock for the anionic systems. In the di-helium species confined in the small C_{60} cage, besides the atomic displacements from the center position, the direct He−He interactions contribute to the ^{3}He shift.

1. Introduction

Helium atom (^{3}He) is an excellent nuclear magnetic resonance (NMR) probe in fullerene chemistry.[1] Inside a fullerene cage it remains chemically inactive, yet it probes the shape, size, and substitution of the fullerene via the helium chemical shift. This allows identifying the endohedral fullerenes as well as their isomers[2,3] and derivatives[4] and following chemical reactions of fullerenes[5] by means of ^{3}He NMR.

The endohedral helium fullerenes can be considered prototypical cases of noble gases confined in cavities. The roles of different factors (cavity size, guest and host dynamics, temperature, etc.) governing the absorption chemical shifts are not fully understood,[6] and there is a demand for computational modeling of such systems. This is not an easy task due to the size of the problem; already the prototypical fullerenes are quite large for quantum-chemical (QC) calculations. Studies of ^{3}He shifts in endohedral fullerenes so far have used the Hartree−Fock (HF) and density functional theory (DFT) approaches.[4,7] Despite their known incapability of describing dispersion forces in weakly bonded systems (as seen, e.g., in erroneous energetics of endohedral fullerenes[8]) both HF and DFT provided qualitatively correct results for the ^{3}He shifts.[4,7] This can be understood because while the dispersion is very important for the interaction energies, interaction-induced NMR shifts in such weakly bonded systems are dominated by overlap effects,[9] in contrast to some old ideas in the field of noble-gas NMR. This is clearly demonstrated, e.g., in work on the Xe dimer by Hanni et al.,[10] where HF calculations with no dispersion reproduce the main part of the interaction-induced shift calculated at the coupled cluster level. While waiting for efficient, highly correlated ab initio methods to become available for the NMR properties of systems of this type, DFT may provide an intermediate solution.

In this work we address the question of how does DFT work for the ^{3}He shifts in the negatively charged endohedral compounds and in cages housing two helium atoms. The NMR data for the $He_n@C_m{}^q$ (n = 1, 2; m = 60, 70, 76, 78; q = 0, 6−) series of fullerenes[2] provide an excellent experimental reference for testing the computational approaches. In particular, does DFT outperform the HF method? Do the methods work for the hexa-anions? Can the quantum-chemical DFT and HF levels account for the small differences (<1 ppm) between the ^{3}He shifts in the di- and mono-helium fullerenes? Here we neglect any dynamic, temperature, and solvent effects and use the affordable BP86/SVP and HF/SVP (cf. see Methods section) levels to model a single molecule at rest at T = 0 K to answer the questions posed above. Additionally, we test methodological aspects using the smallest system, $He@C_{60}$. We are particularly interested in the effects of the choice of the basis set and functional.

* To whom correspondence should be addressed. Fax: (+ 358) 9 191 50 279. E-mail: michal.straka@helsinki.fi, juha.t.vaara@helsinki.fi.

2. Methods

Turbomole,[11] Gaussian 03,[12] and the Mainz−Austin−Budapest version of ACES II[13] codes were employed in the calculations. The energy convergence criteria were set equal to 10^{-8} au in all calculations. The default optimization criteria in Turbomole were tightened by an order of magnitude. The quality of the numerical DFT grid in the NMR calculations was set to “grid = ultrafine” in Gaussian and “gridsize = m5” in Turbomole. Throughout the work we used the BP86,[14,15] BLYP,[14,16] B3LYP,[16,17] BHLYP,[18] PBE,[19] and PBE0[20] density functionals. The SVP,[21] TZVP, TZVPP, and TZVPPP[22] as well as the aug-cc-pVQZ[23] basis sets were employed. It is not known experimentally where the helium atoms reside in the cage. The optimizations started from a structure with the helium atom at the center of mass for the mono-helium species and symmetrically around the center of mass with He−He distance of 200 pm for the di-helium species. The symmetry of each system was maintained during optimization. This was not possible for $He_2@C_{60}{}^q$, where the I_h symmetry is lowered. Preliminary calculations indicate that the two helium atoms move freely in the cage while retaining a He−He distance of about 200 pm. We used the D_{5d} isomer for both $He_2@C_{60}$ and $He_2@C_{60}{}^{6-}$ in which the He−He internuclear axis passes through the opposite pentagon centers.

Helium shifts were obtained with respect to the free helium atom similarly to the experiments. To reduce the basis set superposition errors, we calculated the shift as the difference between the shielding of the reference helium atom in the basis

10.1021/jp0638991 CCC: $33.50
Published on Web 10/12/2006

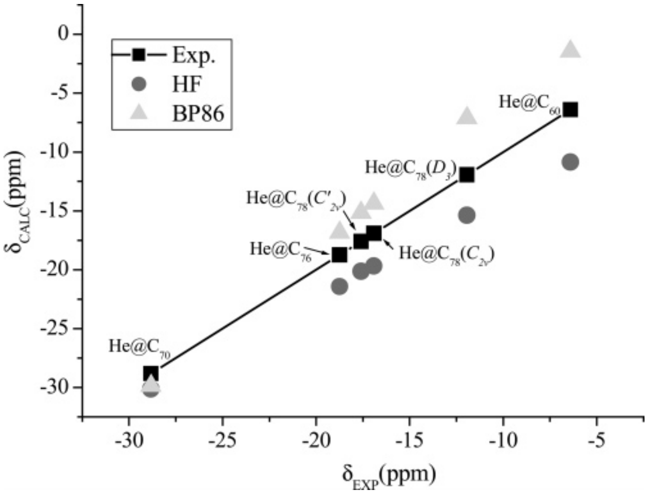

Figure 1. Calculated vs experimental ^{3}He shifts for neutral endohedral fullerenes. Numerical values are listed in Table 1.

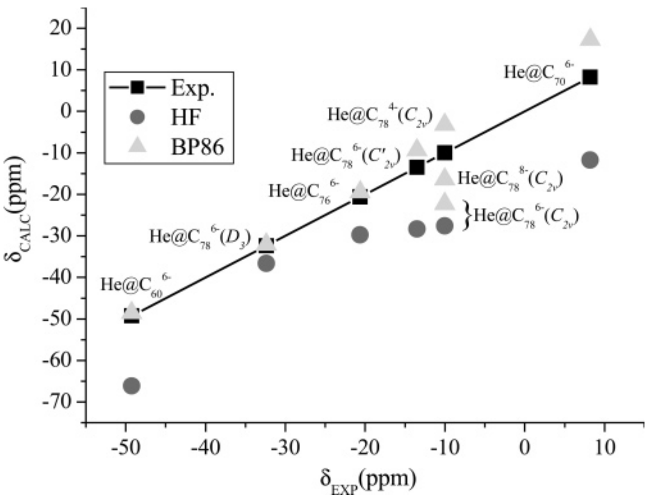

Figure 2. Calculated vs experimental ^{3}He shifts for anionic endohedral fullerenes. Numerical values are listed in Table 1.

set of the full system (setting the carbon charges equal to zero) and the shielding of the helium nucleus in the molecule.

3. Results and Discussion

3.1. Mono-Helium Fullerenes. Figures 1 and 2 and Table 1 show the calculated and experimental ^{3}He shifts for the neutral ($q = 0$) and anionic ($q = 6-$) fullerenes using the BP86/SVP-optimized structures. Though deviations from experiment occur (Table 1), both DFT and HF reproduce the trends systematically (Figures 1 and 2). While DFT overestimates the ^{3}He shift, HF underestimates it, as found earlier.[4] This discrepancy with the experiment increases toward the more positive shifts. The DFT performance is clearly superior for the anions but does not present an improvement over HF for the neutral species. The data for the C_{2v} isomer of the He@C_{78}^{6-} anion does not fit to the general trend in Figure 2. Calculations reveal that the closed-shell hexa-anion is triplet unstable; it is energetically 0.87 au above a triplet ground state. Closer inspection of the He@C_{78}^{6-} (C_{2v}) orbitals suggests that the system is likely to be a tetra-anion. The calculated He@C_{78}^{4-} (C_{2v}) has a singlet ground state, energetically 0.72 au below the singlet hexa-anion. The calculated ^{3}He shift in the tetra-anion (−3.22 ppm) matches the trend in Figure 2 better. The octa-anion He@C_{78}^{8-} with ^{3}He shift of −16.36 ppm is high in energy. On the basis of these calculations, it appears possible that experimentalists have seen the signal of He@C_{78}^{4-} instead of He@C_{78}^{6-} (C_{2v}). With the tetra-anion, all trends in Figures 1 and 2 are systematic.

3.2. Di-Helium Fullerenes. The calculated and experimental shifts for di-helium species are listed in Table 2. Table 3 further shows the calculated as well as the experimental results for the ^{3}He shift differences between the di- and mono-helium species. The experimental differences are quite small, up to 0.15 ppm in magnitude.[2] The origin of the differences may be hard to trace computationally as, e.g., solvent or dynamical effects could contribute such tiny changes. Although the calculated numbers are far from perfect, in all cases but one at least the sign if not the size of this small effect is reproduced. Error cancellation clearly helps here as the deviations of the calculated total ^{3}He shifts (Tables 1 and 2) from experiment are an order of magnitude larger than the shift differences in Table 3. The calculations suggest that the effect of the other helium is already seen at these QC levels. While these data are to be proven by more accurate calculations, it can nevertheless be concluded at least for the larger fullerenes that the DFT and HF methods reproduce the sign of the difference between mono- and di-helium species. Hence, calculations of this change can help in identifying various fullerenes and their isomers.

The differences between ^{3}He@C_n and $^3He_2$@C_n shifts can be negative, positive, or close to zero.[2,24] It has been suggested that the differential shift in di-helium fullerenes is due to the displaced position of He atoms inside the cage as compared to the mono-helium species. This, in turn, results from variation of the magnetic field inside the cage.[2] We carried out BP86/SVP calculations of quasi di-helium systems from which one helium atom is removed and the other remains in the position appropriate to di-helium. The results (Table 2, in parentheses) give strong support to the idea. One may nevertheless ask about the contributions to the ^{3}He shift from the direct interaction of the two heliums in the cage. This can be calculated for the He−He system in free space as a function of the He−He distance. Figure 3 shows the calculated binary ^{3}He shift function $\delta_{He} = \sigma(He_1) - \sigma(He_2)$. Indeed, the ^{3}He shift due to the He−He interaction, calculated at the very accurate CCSD(T)/aug-cc-pVQZ level, is rather small (<0.01 ppm) for the larger fullerenes with longer He−He distances. However, the He−He interaction is relatively important in He_2@C_{60}^{6-} and He_2@C_{60} (the satellite peak for He_2@C_{60} is not resolved on the experimental scale,

TABLE 1: Calculated and Experimental ^{3}He Shifts (ppm) in the Mono-Helium Fullerenes

	δ(neutral, $q = 0$)			δ(anion, $q = 6-$)		
system	HF/SVP	BP86/SVP	exp.[a]	HF/SVP	BP86/SVP	exp.[a]
He@C_{60}^q(I_h)	−10.86	−1.46	−6.40	−66.16	−48.55	−49.27
He@C_{70}^q(D_{5h})	−30.14	−29.86	−28.82	−11.72	+17.31	+8.20
He@C_{76}^q(D_2)	−21.43	−16.85	−18.75	−29.76	−19.51	−20.62
He@C_{78}^q(C_{2v})	−19.68	−14.38	−16.91	−27.57	−22.26[b]	−10.02
He@C_{78}^q(D_3)	−15.38	−7.12	−11.94	−36.64	−32.05	−32.39
He@C_{78}^q(C'_{2v})	−20.14	−15.16	−17.60	−28.34	−9.37	−13.50

[a] Reference 2. [b] Tetra-anion: −3.22 ppm. Octa-anion: −16.36 ppm.

TABLE 2: Calculated and Experimental ^{3}He Shifts (ppm) in the Di-Helium Fullerenes

system	δ(neutral, $q = 0$)			δ(anion, $q = 6-$)		
	HF/SVP	BP86/SVP[b]	exp.[a]	HF/SVP	BP86/SVP[b]	exp.[a]
$He_2@C_{60}{}^q(I_h,D_{5h})$	−10.86	−1.07(−1.31)		−66.19	−48.40(−48.26)	−49.17
$He_2@C_{70}{}^q(D_{5h})$	−30.04	−30.12(−30.09)	−28.81	−12.49	16.74(16.74)	8.04
$He_2@C_{76}{}^q(D_2)$	−21.20	−16.58(−16.56)	−18.61	−29.96	−19.30(−19.30)	−20.55
$He_2@C_{78}{}^q(C_{2v})$	−19.58	−13.82(−13.81)	−16.79	−27.69	−21.88(−21.92)	
$He_2@C_{78}{}^q(D_3)$	−15.40	−6.71(−6.68)		−37.50	−32.35(−32.36)	−32.54
$He_2@C_{78}{}^q(C'_{2v})$	−19.93	−14.37(−14.35)	−17.45	−29.03	−10.06(−10.05)	−13.61

[a] Reference 2. [b] Numbers in parentheses are for the mono-helium species with the helium atom displaced to the position appropriate to the di-helium system.

TABLE 3: Calculated and Experimental Differences[b] between ^{3}He Shifts (ppm) in the Di- and Mono-Helium Fullerenes

system ($n = 1,2$)	Δ^b(neutral, $q = 0$)			Δ^b(anion, $q = 6-$)		
	HF	BP86	exp.[a]	HF	BP86	exp.[a]
$He_n@C_{60}{}^q(I_h)$	+0.00	+0.39		−0.03	+0.15	+0.10
$He_n@C_{70}{}^q(D_{5h})$	+0.10	−0.26	0.01	−0.77	−0.57	−0.16
$He_n@C_{76}{}^q(D_2)$	+0.23	+0.27	0.14	−0.20	+0.21	+0.07
$He_n@C_{78}{}^q(C_{2v})$	+0.10	+0.56	0.12	−0.12	+0.38	
$He_n@C_{78}{}^q(D_3)$	−0.02	+0.41		−0.86	−0.30	−0.15
$He_n@C_{78}{}^q(C'_{2v})$	+0.21	+0.79	0.15	−0.69	−0.69	−0.11

[a] Reference 2. [b] $\Delta = \delta(He_2) - \delta(He_1)$.

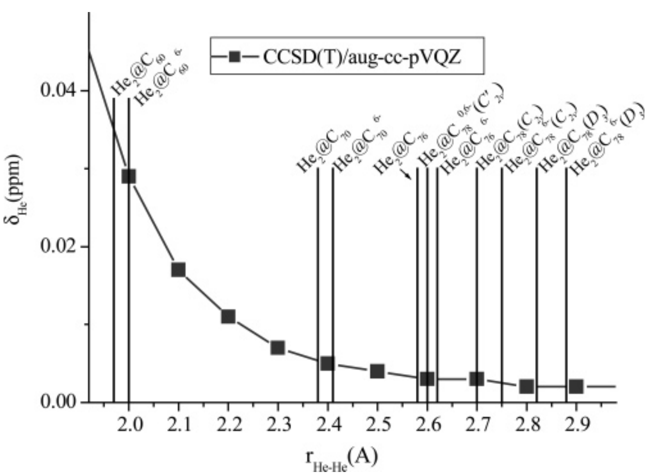

Figure 3. Calculated dependence of ^{3}He shift on the He−He distance in the He−He system. The vertical lines correspond to the optimized He−He distances (at BP86/SVP level) occurring in endohedral fullerenes.

presumably due to a very small shift difference). The CCSD(T)/aug-cc-pVQZ value of 0.03 ppm represents about 30% of the total experimental difference (0.1 ppm, Table 3) between the $He_2@C_{60}{}^{6-}$ and $He@C_{60}{}^{6-}$ helium shifts. Thus, the effects of the He−He interactions on the ^{3}He shift in the di-helium species cannot be neglected in cases when the two helium atoms are close to each other as, e.g., in the C_{60} cage.

3.3. Method Validation Using He@C$_{60}$ Model. We will now study in more detail the He@C_{60} system to gain insight in how to improve the accuracy of QC calculations. He@C_{60} is the computationally lightest system, but it also provides a case with large deviation from the observed ^{3}He shift (Figure 1). While no experiment exists for the structure of He@C_{60}, it can be directly compared with the data for the empty C_{60} cage[25] as the calculations indicate that the C_{60} cage remains unchanged upon insertion of the helium atom.[8a,26]

Of various tested basis sets and density functionals (cf. Methods section), we obtained the best He@C_{60} and C_{60} structures at the BP86/TZVP level. The calculated C−C distances[27] of 140.0 and 145.5 pm are within 0.3 pm from the C_{60} experiment[25] (140.1 and 145.8 pm) and within 0.2 pm from the basis set limit (139.8 and 145.3 pm) estimated from a BP86/TZVPPP calculation. The HF/TZVP structure (136.9 and 144.8 pm) is far from the experimental one. The MP2/TZVP (140.5 and 144.5 pm) and the barely affordable MP2/TZVPPP (140.2 and 144.1 pm) levels give less accurate He@C_{60} structure.

Table 4 lists the ^{3}He shifts calculated using selected DFT functionals as well as with the HF and MP2 approaches. Interestingly, the pure DFT functionals with no exact exchange admixture (BP86, BLYP, PBE) and the ab initio MP2 method provide similar helium shifts, about 6 ppm less shielded than the experimental value. Hartree−Fock (100% exact exchange but no correlation) gives about −9 ppm. As HF and pure DFT bracket the experimental result from both directions, when some percentage of the exact exchange is included in a hybrid functional (B3LYP, 20%; PBE0, 25%; BHLYP, 50%), the calculated shifts improve toward the experiment. For a property significantly affected by the overlap of the monomer wave functions such sensitivity on the admixture of the exact exchange is expected. The best DFT results around −6 to −5 ppm are obtained at the BHLYP level.[28] Apparently, exact exchange reduces the shift while correlation influences it in the opposite direction. This implies that suitable admixture of exact exchange

TABLE 4. Calculated ^{3}He Chemical Shifts (ppm) in He@C$_{60}$

method	structure		
	BP86/TZVP	exp.	method/TZVP[a]
HF	−9.09	−9.34	−11.07
MP2	−0.57	−0.87 (−3.04[b])	+1.76
BP86	−0.48(−1.46,[b] +0.65[c])	−0.58	−0.48
BLYP	−0.67	−0.74	−0.70
B3LYP	−2.71	−2.95	−3.50
BHLYP	−5.34	−5.61(−7.68,[b] −5.58,[c] −5.90[d])	−6.20
PBE	−0.03	−0.02	
PBE0	−3.16	−3.21	
exp.	−6.40		

[a] Structure at the same level as shift. [b] Using SVP basis set. [c] Using TZVPP basis set. [d] Using TZVPPP basis set.

in the functional could be used to empirically tune the DFT results to reproduce experiment for endohedral fullerenes.[28]

The basis set effects are less substantial than those of the choice of the functional. Extending the basis set at the BP86 level takes the shifts further away from the experiment, implying that we benefit from error cancellation (Table 4). At the BHLYP level, quoting the experimental geometry, the largest affordable basis set, TZVPPP, gives −5.90 ppm, about 0.3 ppm below the TZVP value (−5.61 ppm) and 1.8 ppm above the SVP result (−7.68 ppm), see Table 4. The basis set convergence of MP2 shifts could only be roughly estimated (due to code limitations[29]) from the SVP and TZVP results (−3.04 and −0.87 ppm).

Regarding the influence of the accuracy of the calculated molecular structure, the ^{3}He shifts obtained at the experimental geometry are very close to those corresponding to the BP86/TZVP-optimized geometry. Both MP2 and HF structures result in larger deviation from the corresponding data obtained using the experimental geometry (Table 4).

4. Conclusions

The present results suggest that both DFT and HF work qualitatively for the ^{3}He shifts in the neutral and anionic endohedral fullerenes. The experimental trends in the studied $He_n@C_m{}^q$ ($n = 1, 2$; $m = 60, 70, 76, 78$; $q = 0, 6-$) series are reproduced at both BP86 and HF levels using an entry-level SVP basis set. While DFT is superior for the total shift in anionic systems, HF performs better for the rather small differences between the neutral di- and mono-helium fullerenes. Being able to reproduce the sign of the difference between the chemical shifts of di- and mono-helium species may turn out to be useful for assigning the different fullerene isomers. Such differences are mainly due to the displaced helium position in the di-helium compound. However, short He−He distances in the C_{60} cage induce significant relative contributions from the direct He−He interaction.

The calculations on $He@C_{60}$ further demonstrate that DFT provides improved optimized structure and, with hybrid functionals, better ^{3}He shift than the HF and MP2 approaches. As error cancellation is at play in the low-level quantum-chemical methods employed in the present study, a more detailed computational investigation of the present series covering both the quantum-chemical aspects (optimized structure, functional, basis set limit) and the role of the dynamics of the He atoms in the cage is in progress.

Acknowledgment. This project was supported by a Marie Curie Intra-European Fellowship within the 6th European Community framework Program. The Emil Aaltonen Foundation is gratefully acknowledged. The authors are with the Finnish Center of Excellence in Computational Molecular Science. J.V. is an Academy Research Fellow of the Academy of Finland. Computational resources were partially provided by the Center for Scientific Computing, Espoo, Finland.

References and Notes

(1) (a) Saunders, M.; Jiménez-Vázques, H. A.; Cross, R. J.; Mroczkowski, S.; Freedberg, D. I. F.; Anet, A. L. *Nature (London)* **1994**, *367*, 257. (b) Saunders, M.; Cross, R. J.; Jiménez-Vázquez, H. A.; Shimshi, R.; Khong A. *Science* **1996**, *271*, 1693.

(2) Sternfeld, T.; Saunders, M.; Cross, R. J.; Rabinovitz, M. *Angew. Chem., Int. Ed.* **2003**, *42*, 3136 and references therein.

(3) (a) Saunders, M.; Jiménez-Vázquez, H. A.; Cross, R. J.; Billups, W. E.; Gesenberg, C.; Gonzalez, A.; Luo, W.; Haddon, R. C.; Diederich, F.; Herrmann, A. *J. Am. Chem. Soc.* **1995**, *117*, 9305. (b) Sternfeld, T.; Hoffman, R. E.; Saunders, M.; Cross, R. J.; Syamala, M. S.; Rabinovitz, M. *J. Am. Chem. Soc.* **2002**, *124*, 8786.

(4) Wang, G.-W.; Zhang, X.-H.; Zhan, H.; Guo, Q.-X.; Wu, Y.-D. *J. Org. Chem.* **2003**, *68*, 6732 and references therein.

(5) (a) Saunders, M.; Jiménez-Vázquez, H. A.; Bangerter, B. W.; Cross, R. J. *J. Am. Chem. Soc.* **1994**, *116*, 3621. (b) Wang, G.-W.; Saunders, M.; Cross, R. J. *J. Am. Chem. Soc.* **2001**, *123*, 256. (c) Rosenthal, D.; Schuster, D. I.; Cross, R. J.; Kong, A. M. *J. Org. Chem.* **2006**, *71*, 1191.

(6) Jokisaari, J. *Prog. NMR* **1994**, *26*, 1.

(7) (a) Bühl, M.; Thiel, W.; Jiao, H.; Schleyer, P. v. R.; Saunders, M.; Anet, F. A. L. *J. Am. Chem. Soc.* **1994**, *116*, 6005. (b) Cioslowski, J. *Chem. Phys. Lett.* **1994**, *227*, 361. (c) Cioslowski, J. *J. Am. Chem. Soc.* **1994**, *116*, 3619. (d) Bühl, M.; van Wüllen, C. *Chem. Phys. Lett.* **1995**, *247*, 63. (e) Bühl, M.; Thiel, W. *Chem. Phys. Lett.* **1995**, *233*, 585. (f) Bühl, M. *Chem.*−*Eur. J.* **1998**, *4*, 734. (g) Bühl, M.; Kaupp, M.; Malkina, O. L.; Malkin, V. G. *J. Comput. Chem.* **1999**, *20*, 91. (h) Chen, Z.; Cioslowski, J.; Rao, N.; Moncrieff, D.; Bühl, M.; Hirsch, A.; Thiel, W. *Theor. Chem. Acc.* **2001**, *106*, 364. (i) Chen, Z.; King, R. B. *Chem. Rev.* **2006**, *105*, 3613.

(8) (a) Bühl, M.; Patchkovskii, S.; Thiel, W. *Chem. Phys. Lett.* **1997**, *275*, 14. (b) Patchkovskii, S.; Thiel, W. *J. Chem. Phys.* **1997**, *106*, 1796.

(9) (a) Adrian, F. J. *J. Chem. Phys.* **2004**, *120*, 8469. (b) Jameson, C. J.; Sears, D. N.; Murad, S. *J. Chem. Phys.* **2004**, *121*, 9581 and references therein.

(10) Hanni, M.; Lantto, P.; Runeberg, N.; Jokisaari, J.; Vaara, J. *J. Chem. Phys.* **2004**, *121*, 5908.

(11) *Turbomole*, Version 5.71: Ahlrichs, R.; Bär, M.; Häser, M.; Horn, H.; Kölmel, C. *Chem. Phys. Lett.* **1989**, *162*, 165.

(12) Frisch, M. J.; Trucks, G. W.; Schlegel, H. B.; Scuseria, G. E.; Robb, M. A.; Cheeseman, J. R.; Montgomery, J. A., Jr.; Vreven, T.; Kudin, K. N.; Burant, J. C.; Millam, J. M.; Iyengar, S. S.; Tomasi, J.; Barone, V.; Mennucci, B.; Cossi, M.; Scalmani, G.; Rega, N.; Petersson, G. A.; Nakatsuji, H.; Hada, M.; Ehara, M.; Toyota, K.; Fukuda, R.; Hasegawa, J.; Ishida, M.; Nakajima, T.; Honda, Y.; Kitao, O.; Nakai, H.; Klene, M.; Li, X.; Knox, J. E.; Hratchian, H. P.; Cross, J. B.; Bakken, V.; Adamo, C.; Jaramillo, J.; Gomperts, R.; Stratmann, R. E.; Yazyev, O.; Austin, A. J.; Cammi, R.; Pomelli, C.; Ochterski, J. W.; Ayala, P. Y.; Morokuma, K.; Voth, G. A.; Salvador, P.; Dannenberg, J. J.; Zakrzewski, V. G.; Dapprich, S.; Daniels, A. D.; Strain, M. C.; Farkas, O.; Malick, D. K.; Rabuck, A. D.; Raghavachari, K.; Foresman, J. B.; Ortiz, J. V.; Cui, Q.; Baboul, A. G.; Clifford, S.; Cioslowski, J.; Stefanov, B. B.; Liu, G.; Liashenko, A.; Piskorz, P.; Komaromi, I.; Martin, R. L.; Fox, D. J.; Keith, T.; Al-Laham, M. A.; Peng, C. Y.; Nanayakkara, A.; Challacombe, M.; Gill, P. M. W.; Johnson, B.; Chen, W.; Wong, M. W.; Gonzalez, C.; Pople, J. A. *Gaussian 03*, Revision C.02; Gaussian, Inc.: Wallingford, CT, 2004.

(13) Stanton, J. F.; Gauss, J.; Watts, J. D.; Szalay, P. G.; Bartlett R. J. with contributions from Auer, A. A.; Bernholdt, D. B.; Christiansen, O.; Harding, M. E.; Heckert, M.; Heun, O.; Huber, C.; Jonson, D.; Jusélius, J.; Lauderdale, W. J.; Metzroth, T.; Ruud, K. and the integral packages: MOLECULE (Almlöf, J.; Taylor, P. R.), PROPS (Taylor, P. R.), and ABACUS (Helgaker, T.; Jensen, H. J. Aa.; Jørgensen, P.; Olsen J.). See also: Stanton, J. F.; Gauss, J.; Watts, J. D.; Lauderdale, W. J.; Bartlett, R. J. *Int. J. Quantum Chem. Symp.* **1992**, *26*, 879. Current version, see: http://www.aces2.de.

(14) Becke, A. D. *Phys. Rev. A* **1988**, *38*, 3098.

(15) Perdew, J. P. *Phys. Rev. B* **1986**, *33*, 8822.

(16) (a) Lee, C.; Yang, W.; Parr, R. G. *Phys. Rev. B* **1988**, *37*, 785. (b) Miehlich, B.; Savin, A.; Stoll, H.; Preuss, H. *Chem. Phys. Lett.* **1989**, *157*, 200.

(17) (a) Becke, A. D. *J. Chem. Phys.* **1993**, *98*, 5648. (b) Stephens, P. J.; Devlin, F. J.; Chabalowski, C. F.; Frisch, M. J. *J. Phys. Chem.* **1994**, *98*, 11623.

(18) Becke, A. D. *J. Chem. Phys.* **1993**, *98*, 1372.

(19) (a) Perdew, J. P.; Burke, K.; Ernzerhof, M. *Phys. Rev. Lett.* **1996**, *77*, 3865. (b) Perdew, J. P.; Burke, K.; Ernzerhof, M. *Phys. Rev. Lett.* **1997**, *78*, 1396.

(20) Adamo, C.; Barone, V. *J. Chem. Phys.* **1999**, *110*, 6158.

(21) Schäfer, A.; Horn, H.; Ahlrichs, R. *J. Chem. Phys.* **1992**, *97*, 2571.

(22) Schäfer, A.; Huber, C.; Ahlrichs, R. *J. Chem. Phys.* **1994**, *100*, 5829.

(23) Woon, D. E.; Dunning, T. H., Jr. *J. Chem. Phys.* **1994**, *100*, 2975.

(24) Wang, G.-W.; Saunders, M.; Khong A.; Cross, R. J. *J. Am. Chem. Soc.* **1994**, *122*, 3216.

(25) Hedberg, K.; Hedberg, L.; Bethune, D. S.; Brown, C. A.; Dorn, H. C.; Johnson, R. D.; de Vries, M. *Science* **1991**, *254*, 410.

(26) This was checked by us up to BP86/TZVPPP and second-order Møller−Plesset perturbation theory (MP2)/TZVPPP levels.

(27) Two unique C−C distances are enough to specify the structure of icosahedral C_{60} and $He@C_{60}$ systems. The shorter distance corresponds to the joint C−C bond of two hexagons and the longer distance to the joint C−C bond of a hexagon and a pentagon.

(28) The BHLYP functional also performs very well in comparison to CCSD(T) for the ^{129}Xe shift in the weakly bonded $Xe\cdots C_6H_6$ model system in our unpublished work.

(29) The MP2 shift calculations are extremely demanding. The MP2/TZVP ^{3}He shift in $He@C_{60}$ took more than 2 weeks using eight AMD Opteron (2.2 GHz) processors in a quasi-parallel calculation.